Cocoon bifurcation in three-dimensional reversible vector fields

Freddy Dumortier
Universiteit Hasselt
Campus Diepenbeek
Agoralaan-Gebouw D, B-3590, Diepenbeek, Belgium
E-mail: freddy.dumortier@uhasselt.be

Santiago Ibáñez*
Department of Mathematics
University of Oviedo
Avda. Calvo Sotelo s/n, 33007 Oviedo, Spain
E-mail: mesa@pinon.ccu.uniovi.es

Hiroshi Kokubu†
Department of Mathematics
Kyoto University
Kyoto 606-8502, Japan
E-mail: kokubu@math.kyoto-u.ac.jp

Dedicated to Robert Roussarie for his sixtieth birthday

September 19, 2005

*Partially supported by the projects FICYT PB-EXP01-29 and MCT-02-BFM-00241.
†Partially supported by Grant-in-Aid for Scientific Research (No.14340055, No.

Abstract

The cocoon bifurcation is a set of rich bifurcation phenomena numerically observed by Lau [17] in the Michelson system, a three-dimensional ODE system describing travelling waves of the Kuramoto-Sivashinsky equation. In this paper, we present an organizing center of the principal part of the cocoon bifurcation in more general terms in the setting of reversible vector fields on $\mathbb{R}^3$. We prove that in a generic unfolding of an organizing center called the *cusp-transverse heteroclinic chain*, there is a cascade of heteroclinic bifurcations with increasing length close to the organizing center, which resembles the principal part of the cocoon bifurcation.

We also study a heteroclinic cycle called the *reversible Bykov cycle*. Such a cycle is believed to occur in the Michelson system, as well as in a model equation of a Josephson Junction ([23]). We conjecture that a reversible Bykov cycle is, in its unfolding, an accumulation point of a sequence of cusp-transverse heteroclinic chains. As a first result in this direction, we show that a reversible Bykov cycle is an accumulation point of reversible generic saddle-node bifurcations of periodic orbits, the main ingredient of the cusp-transverse heteroclinic chain.

1 Introduction

There are a number of papers devoted to studying the dynamics and bifurcations of the following one-parameter family of vector fields on $\mathbb{R}^3$ (e.g. [5, 11, 12, 13, 17, 19, 20, 22, 24]):

$$\begin{aligned} \dot{x} &= y \\ \dot{y} &= z \\ \dot{z} &= c^2 - \tfrac{x^2}{2} - y. \end{aligned} \tag{1.1}$$

On one hand, this system appears as a part of the limit family of the unfolding of the nilpotent singularity of codimension three (see [5]) given by the following equations:

$$\begin{aligned} \dot{x} &= y \\ \dot{y} &= z \\ \dot{z} &= \lambda + \mu y + \nu z + x^2, \end{aligned} \tag{1.2}$$

17340045), Ministry of Education, Science, Technology, Culture and Sports, Japan.

where $(\lambda, \mu, \nu) \in S^2$. When $\nu = 0$, $\lambda \leq 0$ and $\mu < 0$, a simple change of coordinates and a reparametrization transforms (1.2) into the family (1.1).

On the other hand, the family (1.1), also called the Michelson system, appears as the equation for travelling wave solutions of a non-linear PDE called the Kuramoto-Sivashinsky equation in one-dimensional media:

$$u_t + u_{xxxx} + u_{xx} + \frac{1}{2}u_x^2 = 0, \quad (t \geq 0, x \in \mathbb{R}).$$

See [12] or [20] for precise derivation of (1.1) from the PDE. Because of this reason, the system (1.1) has attracted much attention for research.

Let us observe some basic properties of (1.1):

- Since the divergence is identically zero, the family is volume-preserving.
- The family is reversible, namely, it is invariant under the involution $R : (x, y, z) \mapsto (-x, y, -z)$ and the time reverse $t \mapsto -t$.
- For $c > 0$ there are only two equilibrium points at

  $$P_\pm = (\pm\sqrt{2}c, 0, 0),$$

  both are of saddle-focus type with $\dim(W^u(P_+)) = \dim(W^s(P_-)) = 2$.

As was pointed out in [20], it follows from the results in [19] that for c large enough there is a unique transverse heteroclinic orbit connecting P_+ and P_- in (1.1) which is given by the intersection of the two-dimensional invariant manifolds, and the equilibrium points together with the heteroclinic orbit form the maximal bounded invariant set of the family (1.1).

When the parameter c decreases, according to the numerical results in [17] and [20], the family exhibits an infinite sequence of heteroclinic bifurcations, each of which creates a pair of new transverse heteroclinic orbits. Again it follows from the numerical results in these papers that the sequence of heteroclinic bifurcations converges to $\bar{c} \approx 1.2662$. For this value, there appears a saddle-node bifurcation that creates a periodic orbit γ_*, symmetric under the involution R and intersecting with the y-axis, which is the fixed point subspace of R. According to [20], the parameter value $\bar{c}$ seems corresponding to the largest value for which a periodic orbit exists. The sequence of bifurcations that appear before and after $c = \bar{c}$ was studied by Lau [17] mainly using careful numerical simulation, and was called the "cocoon" bifurcation, because of the specific shape of the invariant manifolds controlling the process, see [17].

The cascade of heteroclinic bifurcations, caused by the tangency of $W^u(P_+)$ and $W^s(P_-)$, and accumulating from above to the parameter value $\bar{c} \approx 1.2662$, has been numerically observed by Lau. Here we call it the "principal sequence" of Lau's cocoon bifurcation.

The goal of this paper is to study this principal sequence from a theoretical and more general point of view, and to explain its occurrence as a consequence of the presence of an organizing center. In order to state our main results precisely, we begin by stating some definitions.

Let X_λ be a one-parameter family of vector fields on $\mathbb{R}^3$ having the following properties:

(H1) Each of the vector fields X_λ is time-reversible with respect to the linear involution R with $\dim(\mathrm{Fix}(R)) = 1$, where $\mathrm{Fix}(R)$ stands for the fixed point subspace of R;

(H2) There exist two hyperbolic equilibrium points $P_\pm \notin \mathrm{Fix}(R)$ which are symmetric under the involution R and such that $\dim W^u(P_+) = \dim W^s(P_-) = 2$.

Remark 1.1 Without loss of generality, one can assume that the linear involution R in (H1) is given by the map $(x, y, z) \mapsto (-x, y, -z)$.

Remark 1.2 We refer to [15] for a quite complete survey and an extensive bibliography about reversible dynamical systems in both continuous and discrete cases.

Definition 1.3 Under the conditions (H1) and (H2), we say the family X_λ exhibits a *cocooning cascade of heteroclinic tangencies* centered at λ_*, if there is a closed solid torus T with $P_\pm \notin T$ and a monotone infinite sequence of parameters λ_n converging to λ_*, for which the corresponding vector field X_{λ_n} has a tangency of $W^u(P_+)$ and $W^s(P_-)$ such that the heteroclinic tangency orbit intersects with T and has its length within T tending to infinity as $n \to \infty$.

Definition 1.4 A family of vector fields X_λ on $\mathbb{R}^3$ satisfying (H1) and (H2) is said to have a *cusp-transverse heteroclinic chain* at $\lambda = \lambda_0$, if the following three conditions hold:

(C1) X_{λ_0} has a saddle-node periodic orbit γ_* which is symmetric under the involution R.

(C2) The saddle-node periodic orbit γ_* is generic and generically unfolded in X_λ under the reversibility with respect to R.

(C3) $W^u(\gamma_*)$ and $W^s(P_-)$, as well as $W^s(\gamma_*)$ and $W^u(P_+)$, intersect transversely, where $W^s(\gamma_*)$ and $W^u(\gamma_*)$ stand for the stable and unstable sets of the non-hyperbolic periodic orbit γ_*.

Note that, because of the reversibility, the saddle-node periodic orbit in (C1) must intersect with $\mathrm{Fix}(R)$ (see [15]).

Our main result is the following:

Theorem 1.5 *Let X_λ be a smooth family of reversible vector fields on $\mathbb{R}^3$ with (H1) and (H2). Suppose at $\lambda = \lambda_0$ the corresponding vector field X_{λ_0} has a cusp-transverse heteroclinic chain. Then the family X_λ exhibits a cocooning cascade of heteroclinic tangencies centered at λ_0.*

Remark 1.6 The name "cusp-transverse" comes from the fact that, under the genericity condition (C2), the Poincaré map along the saddle-node periodic orbit has a fixed point whose stable and unstable sets form a cusp, see Figure 1 in Section 2, and by the condition (C3) they intersects the unstable and stable manifolds of the equilibrium points $P_\pm$ transversely. Under the bifurcation, the saddle-node periodic orbit will split into two periodic orbits for λ on one side of λ_*, while no periodic orbit will be present near γ_* for λ on the other side of λ_*. The cocooning cascade occurs for the latter values of λ. Geometric structure of the cusp-transverse heteroclinic chain will become clear once the local structure of the saddle-node periodic orbit is studied in Section 2. See Figure 3 as representing a crucial part of the structure.

Remark 1.7 We briefly illustrate how the generic saddle-node periodic orbit implies the cusp structure in the case of (1.1). The family (1.1) is reversible under the linear involution $R : (x, y, z) \mapsto (-x, y, -z)$ whose fixed point subspace is the y-axis, hence one-dimensional. Suppose at a parameter value $\lambda = \lambda_0$, there is a saddle-node periodic orbit γ which is invariant under R and hence intersects with the y-axis. Denote by Π the Poincaré map along γ at a point $p = (0, y_0, 0)$ in $\mathrm{Fix}(R)$. Notice that p is a fixed point of Π. Since the vector field is reversible, by choosing the (y, z)-plane as an invariant cross section under R, one sees that Π is also reversible, namely it is conjugate to its inverse by the restricted involution. In particular, the determinant of $D\Pi(p)$ at the fixed point p is equal to 1, because the Poincaré map is

flow-defined, hence orientation preserving. Knowing that 1 is an eigenvalue of $D\Pi(p)$ as p is a saddle-node fixed point, we conclude that 1 is a double eigenvalue of $D\Pi(p)$. Moreover, we assume that the eigenvalue 1 is not semi-simple, which is a generic condition under the presence of saddle-node. This fact is supported by a numerical result in Section 4 for (1.1). It follows that the linear part of Π is conjugate to the unipotent matrix

$$\begin{pmatrix} 1 & 1 \\ 0 & 1 \end{pmatrix}. \tag{1.3}$$

In the analysis developed in Section 2, a reversible diffeomorphism with the unipotent linear part at a fixed point is studied through a nilpotent singularity of a planar reversible vector field. By using the blow up technique, we can show that the stable and unstable sets of the fixed point of Π indeed form a cusp structure.

Remark 1.8 The description of "cocoon bifurcations" in Lau's paper [17] is phenomenological, in the sense that a list of dynamical behaviors and their changes (bifurcations) with variation of the parameter c is given in relation to associated changes in the structure of numerically computed stable and unstable manifolds of equilibrium points. Our motivation was to treat these complex bifurcation phenomena by a general and solid mathematical manner. Theorem 1.5 says that at least a part of it, namely the accumulation of infinitely many heteroclinic tangency bifurcations, can be understood as a consequence of the presence of a cusp-transverse heteroclinic chain. Therefore one can understand that such a sequence of heteroclinic bifurcations in the description of Lau's cocoon bifurcation is not a special bifurcation phenomenon which occurs only in the Michelson system. Indeed, it will be shown that the same phenomena indeed occurs in a different system.

We believe that other part of the Lau's cocoon bifurcations can also be understood from this point of view, but this will be the subject of future work.

In order to rigorously show the existence of a cusp-transverse heteroclinic chain in a given family of vector fields, one must verify the conditions (C1-C3), which is in general not easy by analytical methods and often requires numerical computation (see Section 4). However, we believe there is a bifurcation mechanism producing cusp-transverse heteroclinic chains.

Definition 1.9 Let X_λ be a family of vector fields on $\mathbb{R}^3$ satisfying (H1) and (H2). A *reversible Bykov cycle* is a heteroclinic cycle in X_{λ_0} for some λ_0 consisting of two heteroclinic orbits between the equilibrium points $P_\pm$, one given by the intersection, and hence coincidence of branches, of one-dimensional invariant manifolds $W^u(P_-)$ and $W^s(P_+)$, and the other given by an intersection of two-dimensional invariant manifolds $W^u(P_+)$ and $W^s(P_-)$. Moreover we assume that the equilibrium points are of saddle-focus type, and that the following non-degeneracy conditions hold:

(B1) The intersection $W^u(P_+) \cap W^s(P_-)$ is transverse;

(B2) As the parameter λ is varied around λ_0, the heteroclinic orbit $W^u(P_-) \cap W^s(P_+)$ unfolds generically, namely the distance between $W^u(P_-)$ and $W^s(P_+)$ measured in a transverse plane is diffeomorphic to $\mu = \lambda - \lambda_0$.

In a general context, not including the reversibility assumption, the coincidence of branches of the one-dimensional invariant manifolds along a heteroclinic orbit Γ is a codimension two phenomenon. On the other hand, since the intersection between the two-dimensional invariant manifolds is transverse, it has codimension zero. Hence, in general, a heteroclinic cycle as described above has codimension two. Nevertheless, when the system is reversible, a heteroclinic orbit Γ exists if and only if $W^u(P_-)$ intersects $\mathrm{Fix}(R)$ and therefore a reversible Bykov cycle has codimension one under reversibility.

Remark 1.10 Since the Michelson system (1.1) is divergence-free, the eigenvalues at $P_- = (-\sqrt{2}, 0, 0)$ satisfy $\lambda_-^u + 2\mathrm{Re}(\lambda_-^s) = 0$, where λ_-^u and λ_-^s are the unstable and stable eigenvalues at P_-, and hence they satisfy the so-called Shil'nikov condition:

$$0 < \frac{|\mathrm{Re}(\lambda_-^s)|}{\lambda_-^u} = \frac{1}{2} < 1.$$

We do not rely on the condition in this paper. However, the dynamics and bifurcations from the reversible Bykov cycle satisfying Shil'nikov condition become richer than those without it since, for instance, the existence of Shil'nikov homoclinic orbits follows. See e.g. [5] and [16].

Remark 1.11 We have chosen the name "Bykov cycle" for the cycle characterized in the above definition, because it was V. V. Bykov in [1] who studied some of the dynamical consequences from the existence of similar

kinds of heteroclinic cycles in a more general context than reversible ones. Some recent results in the general context can also be found in [8]. This type of heteroclinic cycle, or rather its bifurcation point, is sometimes called a "T-point" [9].

An explicit heteroclinic solution representing a coincidence of one-dimensional branches has been found (see [13]) in the Michelson system (1.1) at the parameter value $c = c_K = 15\sqrt{22/19^3}$. Then by showing the topological transversality of the two-dimensional invariant manifolds of these equilibrium points [11], a heteroclinic cycle indeed exists in (1.1) at this parameter value. This heteroclinic cycle almost satisfies the definition of the reversible Bykov cycle, but it remains to verify the genericity conditions (B1) and (B2), which might be tractable by rigorous numerical computation.

We have the following

Conjecture *Let X_λ be a family of vector fields with (H1) and (H2). Suppose at λ_∞ the vector field X_{λ_∞} has a reversible Bykov cycle. Then, there exist two sets of infinite sequences of parameters $\{\lambda_n^\pm\}_{n\in\mathbb{N}}$ with $\lambda_n^- < \lambda_\infty < \lambda_n^+$, converging to λ_∞ as $n \to \infty$, such that each $X_{\lambda_n^\pm}$ has a cusp-transverse heteroclinic chain.*

Remark 1.12 In view of Theorem 1.5, this conjecture asserts that there is an infinite set of "cocoon" bifurcations accumulating at the reversible Bykov cycle. This is stronger than the mere accumulation of heteroclinic bifurcations (the cocooning cascade of heteroclinic tangencies). In other words, the conjecture indicates a nested structure of bifurcations where heteroclinic tangencies accumulate to saddle-node periodic orbits which in turn accumulate to a reversible Bykov cycle.

At the moment, we are not able to prove the conjecture. In Section 3, we will, however, prove the following theorem:

Theorem 1.13 *Let X_λ be a smooth one-parameter family of vector fields with (H1) and (H2). Suppose at λ_∞ the vector field X_{λ_∞} has a reversible Bykov cycle. Then there exist two sets of infinite sequences of parameters $\{\lambda_n^\pm\}_{n\in\mathbb{N}}$ with $\lambda_n^- < \lambda_\infty < \lambda_n^+$, converging to λ_∞ as $n \to \infty$, such that each $X_{\lambda_n^\pm}$ has a saddle-node periodic orbit satisfying the conditions (C1) and (C2).*

Remark 1.14 We consider this theorem as a first attempt to proving the above conjecture, since the existence of a saddle-node periodic orbit with the conditions (C1) and (C2) is the main ingredient of the cusp-transverse heteroclinic chain. Proving the condition (C3) seems to be a more involved task. In order to achieve such a goal one has to understand how the stable and unstable sets of the saddle-node periodic orbits evolve when they approach the reversible Bykov cycle. More precisely, we need a result showing that, after choosing an appropriate transverse section Σ, they tend to $W^s(P_-) \cap \Sigma$ and $W^u(P_+) \cap \Sigma$, respectively. This requires further investigation.

Remark 1.15 Bifurcations from a reversible Bykov cycle are studied extensively by Lamb et al. [16], where they proved, among other things, bifurcations of countably many homoclinic and heteroclinic orbits from the cycle. Such heteroclinic orbits may be related to the ones expected from the above Conjecture. On the other hand, although it is not explicitly mentioned, it also follows from the results in [16] that there exist two sequences of parameters, converging to λ_∞, where the family shows a saddle-node bifurcation. In fact, the bifurcation equation from which we directly derive the existence of such sequences can also be found there in an equivalent formulation. Nevertheless, there is no argument in [16] leading to the genericity condition (C2), which is essential in the proof of our main result.

In [23], the existence of a one-dimensional saddle-saddle connection is proven for a model equation of the Josephson Junction, and the transversality of two-dimensional invariant manifolds is numerically verified, without rigurous error estimate. Noticing that the model equation is reversible under a suitable linear involution, these results show the presence of a reversible Bykov cycle in the model equation, and therefore, from the results of this paper, it is very likely that the cusp-transverse heteroclinic chains and accompanying cocooning cascades of heteroclinic tangencies should exist in this system, similarly to the Michelson system and probably in many others.

The structure of the rest of this paper is as follows: In Section 2, we consider a one-parameter family of reversible diffeomorphisms f_λ such that f_0 has a fixed point with the unipotent matrix as its linearization. Using results obtained in [14], we will see that, under generic assumptions, such a family can be written, up to infinite order, as the time-one mapping associated to a family of vector fields unfolding the planar nilpotent singularity of codimension two. From this fact and the transversality of the invariant manifolds,

we give a proof of Theorem 1.5. Theorem 1.13 is proven in Section 3. In Section 4, we show numerical results which support and illustrate many of the theoretical results as well as the conjecture given in the paper.

We would like to thank the referees for their valuable remarks and suggestions concerning an earlier version of this paper; they helped improving the presentation.

2 Study of planar reversible diffeomorphisms near a fixed point with unipotent linear part

2.1 Formal embedding of a reversible diffeomorphism in a flow

Consider a C^∞ one-parameter family of diffeomorphisms f_λ on the plane, with $f_0(0,0) = (0,0)$ and $Df_0(0,0)$ given by (1.3). Moreover assume that each f_λ is reversible with respect to $R(x,y) = (x,-y)$, namely $R \circ f_\lambda \circ R = f_\lambda^{-1}$.

Remark 2.1 Attention should be paid to the notation here. Throughout the paper, the variables of the two-dimensional Poincaré maps derived from reversible vector fields are (y,z). Only in this section, in order to formulate general results, we will use x and y, playing the same role as y and z in other sections.

We will consider λ as a third variable and define f as the germ at 0 of the C^∞ diffeomorphism in $\mathbb{R}^3$ given by

$$f : (x,y,\lambda) \to f(x,y,\lambda) = (f_{\lambda,1}(x,y), f_{\lambda,2}(x,y), \lambda),$$

where $f_{\lambda,1}$ and $f_{\lambda,2}$ denote the components of f_λ. In the next theorem we will see how f can be embedded in the flow of a vector field on $\mathbb{R}^3$ having family character with respect to the third variable in the sense of the following definition.

Definition 2.2 Let g be the germ at $(0,0)$ of a C^∞ diffeomorphism in $\mathbb{R}^n \times \mathbb{R}^m$, with $g(0,0) = (0,0)$ and $P \circ g = P$, where $P : \mathbb{R}^n \times \mathbb{R}^m \to \mathbb{R}^m$ denotes

the natural projection. Let X be a C^∞ vector field on $\mathbb{R}^n \times \mathbb{R}^m$ such that $X(0) = 0$ and $P \circ X = 0$. We say that g *formally embeds as a family in the flow* of X if there exists a C^∞ diffeomorphism ψ in $\mathbb{R}^n \times \mathbb{R}^m$, with $\psi(0,0) = (0,0)$ and $P \circ \psi = P$, such that the infinite jets of $\psi^{-1} \circ g \circ \psi$ and of the time-one mapping of X coincide at 0.

Let us state the following theorem without proof. A proof can be obtained based on [21], together with some straightforward calculation exploiting the reversibility. A more specified expression can be found in [14], but we do not need to rely on it.

Theorem 2.3 *Assume that* $\frac{\partial f_2}{\partial \lambda}(0) \neq 0$ *and* $\frac{\partial^2 f_2}{\partial x^2}(0) \neq 0$. *Then, up to a* λ*-dependent* C^∞ *coordinate change in the* (x,y)*-plane and a regular reparametrization in* λ, f *formally embeds as a family in the flow of a* C^∞ *vector field:*

$$X : \begin{cases} x' &= y \\ y' &= \lambda + m(\lambda)x + x^2 + x^3 g(x,\lambda) \\ & \quad + y(k(\lambda) + l(\lambda)x + x^2 h(x,\lambda)) + y^2 Q(x,y,\lambda) \\ \lambda' &= 0, \end{cases} \tag{2.1}$$

with $m(0) = k(0) = 0$.

2.2 Study of the germ f_λ at the zero-parameter value

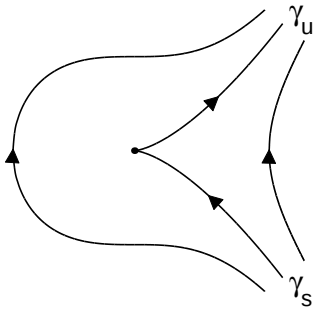

Figure 1: Phase portrait of X_0.

This kind of germ of the diffeomorphism given above has been studied in [6], where the following theorem has been proven:

Theorem 2.4 *Let f_0 be a C^∞ germ having a 1-jet $j_1 f(0) = \mathrm{id} + N$, where N is nilpotent and non-zero, and a generic 2-jet in the sense of Theorem 2.3. Then f_0 embeds in a C^∞-way in the flow associated to a generic cusp-like vector field as its time-one map. As an additional consequence, there exist a stable branch γ_s and an unstable branch γ_u emanating from $(0,0)$.*

Let us quickly repeat some steps in the proof of this theorem, and add some extra information in view of the rest of the construction.

The related vector field can be given in the traditional smooth normal form for nilpotent vector fields:

$$y\frac{\partial}{\partial x} + (\alpha(x) + y\beta(x) + y^2\gamma(x,y))\frac{\partial}{\partial y},$$

where $\gamma(x,y)$ has vanishing infinite jet at $(0,0)$, $\beta(0) = 0$, $\alpha(0) = \alpha'(0) = 0$, and, because of the conditions in Theorem 2.3, $\alpha''(0) \neq 0$. As such the phase portrait of the vector field X_0 is as given in Figure 1. Here we note that, in this subsection, we consider the vector field X as a family of two-dimensional vector fields parametrized by λ, and we use the notation X_λ for indicating it. The above X_0 is therefore understood as the planar vector field at $\lambda = 0$.

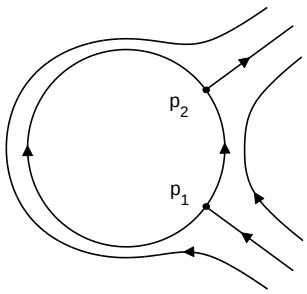

Figure 2: Blow-up of X_0.

The "phase portrait" of f_0 is similar to the one in Figure 1, in the sense that the orbits of f_0 respect the orbit structure of such a nilpotent cusp-type singularity. It for instance makes sense to talk about a stable branch γ_s and an unstable branch γ_u emanating from the origin. The proof of Theorem 2.4 is based on a blow-up procedure

$$(x,y) = (r^2\cos\theta, r^3\sin\theta). \tag{2.2}$$

This blow-up can be applied both to f_0 and to X_0, and in studying the vector field X_0 we can even rescale time by a factor $1/r$, so that we get a desingularized situation as depicted in Figure 2.

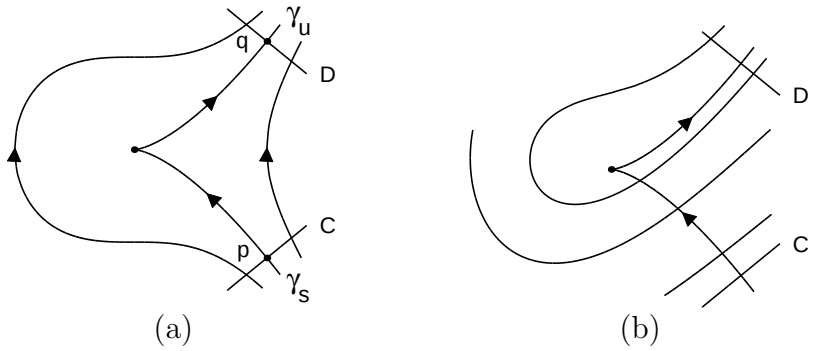

Figure 3: Iterates of segments transverse to γ_s.

In Figure 2 the two singularities p_1 and p_2 on the singular locus $\{r = 0\}$ are hyperbolic saddles. The two invariant curves γ_s and γ_u are obtained by blowing-down the respective stable manifold of p_1 and unstable manifold of p_2. Of course in blowing-up f_0 we can not rescale time and the dynamics of the blown-up diffeomorphism $\hat{f}_0$ are essentially as depicted in Figure 2, with the exception that $\hat{f}_0 \mid \{r = 0\}$ is the identity.

Suppose that some dynamically relevant one-dimensional manifold, like the intersection of the (x, y)-plane with the two-dimensional unstable manifold of the equilibrium point P_+ of the three-dimensional flow, cuts γ_s transversely at some point p, like in Figure 3(a); let us only consider a segment C of the manifold which is everywhere transverse to the vector field X_0. We similarly consider some segment D, transverse to X_0 and cutting γ_u at some point q; it could belong to some dynamically relevant one-dimensional manifold, like the intersection of the (x, y)-plane with the two-dimensional stable manifold of the equilibrium point P_- of the three-dimensional flow.

Theorem 2.5 *Let f_λ be a C^∞ family of planar diffeomorphisms as in Theorem 2.3. We suppose that f_λ is reversible under the mapping $R : (x, y) \mapsto (x, -y)$, namely $R \circ f_\lambda \circ R = f_\lambda^{-1}$.*

Consider invariant curves γ_s and γ_u for f_0 as obtained in Theorem 2.4. Let C be a segment transversely cutting γ_s at some point $p_1 \in \gamma_s$ and let D

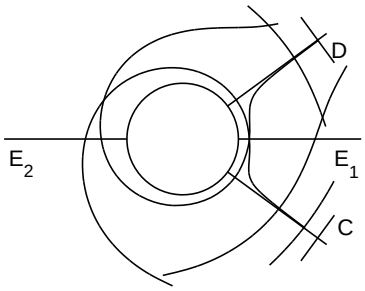

Figure 4: Iterates of C and D after blowing-up.

be its mirror image under R transversely cutting γ_u at p_2, where γ_u and p_2 are the mirror images of γ_1 and p_1 under R, respectively.

Then, for N sufficiently large, the iterates $f_0^N(C)$ and $f_0^{-N}(D)$ cut each other as represented in Figure 5.

PROOF. In studying forward iterates of C and backward iterates of D, we have to restrict to discrete iterates in working with f_0, but for X_0 we can permit to work with continuous time-t iterates. Let us first keep D fixed and only follow C in forward time.

We will show that the iterates behave like in Figure 3(b), i.e., they start bending around the singularity and after a while start cutting D, in a transverse way, exactly twice.

The proof is again based on the blow-up (2.2), but since the original time is important in the construction, we are not allowed to rescale by a factor $1/r$. The blown-up vector field is hence essentially like in Figure 2, except for the fact that $\hat{X}_0 \mid \{r = 0\} \equiv 0$; the desingularized picture, as drawn in Figure 2, can only be obtained by considering $\bar{X}_0 = \frac{1}{r}\hat{X}_0$. In Figure 4 we draw the blown up situation representing C and D in it, without changing the notation, and introducing extra segments E_1 and E_2. What we have to use in between C and E_1 (resp. E_2) and in between E_1 (resp. E_2) and D, is a kind of λ-lemma type argument, in the presence of a hyperbolic saddle with an extra time-degeneracy. This has been studied in [3] and [6]. In [3] it has been proven that the transit time of $\hat{X}_0$ in between C and $E_{1,2}$ (and equally in between D and $E_{1,2}$) is monotonically going to ∞ when the orbits approach the singular locus $\{r = 0\}$.

Let us continue reasoning with C and E_1; the other situations dealing with D or E_2 are similar. For t sufficiently large, the iterates $\hat{X}_{0,t}(C)$ will cut

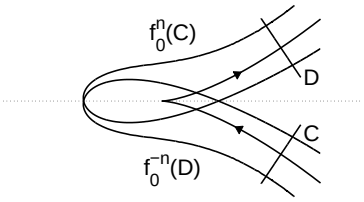

Figure 5: Iterates of C and D in a time-reversible situation.

E_1 at a unique point p_t in a way that their tangent line at p_t makes a nonzero angle with $\hat{X}_0(p_t)$. If we can prove that this angle tends to zero for $t \to +\infty$, or equivalently for $p_t \to 0$, then it will follow that the $\hat{X}_0$-iterates of C over a positive time will cut the $\hat{X}_0$-iterates of D over a negative time exactly once on the E_1 side and once on the E_2 side; the intersection will be transverse. This type of λ-lemma argument is commonly used in hyperbolic situations but requires a proof in this more degenerate situation. The calculations to be made are completely similar to the ones that have been performed in [4] in a more degenerate semi-hyperbolic case.

This observation at the time-t iterates of C and D for the vector field $\hat{X}_0$ of course applies to the discrete iterates for $\hat{f}_0$ giving a similar picture as in Figure 4.

If we apply this result to the original f_0 then we can also use the fact that f_0 is "time-reversible" under the mapping $(x, y, n) \to (x, -y, -n)$. As such γ_u is obtained from γ_s by the reflection $(x, y) \to (x, -y)$. Since the invariant manifolds that we are interested in are in a symmetric position with respect to $\{y = 0\}$, we can, in the previous construction, also restrict to some segment D, which is obtained from C by the reflection $(x, y) \to (x, -y)$. For $n \geq 0$ sufficiently large, the iterates $f_0^n(C)$ and $f_0^{-n}(D)$, restricted to some neighbourhood of $(0, 0)$, will be like in Figure 5, with $f_0^n(C)$ and $f_0^{-n}(D)$ mirror images under $(x, y) \to (x, -y)$. The angles between $f_0^n(C)$ and $f_0^{-n}(D)$ along the x-axis are necessarily like in the figure. In fact any different situation would either lead to tangencies or to extra intersections, which are both excluded by the previous construction. $\square$

2.3 Study of the germ of the family f_λ

We will continue using the notations introduced in the previous paragraph.

Theorem 2.6 *Under the same hypotheses as in Theorem 2.5, there exists a sequence of parameter values $\lambda_n \downarrow 0$ such that for each λ_n there is some N_n such that $f_{\lambda_n}^{N_n}(C)$ and $f_{\lambda_n}^{-N_n}(D)$ have a point of tangency. Moreover, $N_n \to \infty$ as $n \to \infty$.*

Like in the proof of Theorem 2.5, we again use blow up but this time in $\mathbb{R}^3$ instead of in $\mathbb{R}^2$. We in fact consider λ to be a third variable, considering the family f_λ as a diffeomorphism on $\mathbb{R}^3$ given by

$$(x, y, \lambda) \to (f_{\lambda,1}(x, y), f_{\lambda,2}(x, y), \lambda),$$

and we will concentrate on the study of its germ at $(x, y, \lambda) = (0, 0, 0)$. As observed in Subsection 2.1, this germ formally embeds in a flow related to an unfolding of a nilpotent singularity. Up to a diffeomorphism respecting λ and a regular reparametrization of λ, we can suppose that as a germ at $(0, 0, 0)$, f_λ is infinitely close to the time-one mapping of some vector field (2.1) with C^∞ functions m, k, l, g, h and Q, $m(0) = k(0) = 0$ and $Q(x, y, \lambda) = O(\|(x, y, \lambda)\|^N)$ with N given a priori and as large as needed. In this expression we use the information obtained in Subsection 2.1. Let us observe that this normal form has more terms than the traditional one where $m(\lambda) = 0$ and $g(x, \lambda) = 0$ for all x and λ. The latter is however valid for C^∞ equivalence, while in the current study we have to rely on C^∞ conjugacies. As formal calculation suggests, we can probably suppose that k, l and h are identically zero, but we will not use this since we do not need it. For further study we now rely on the results in [7], indicating the different steps in the procedure, but leaving the technical details to [7]. The construction is based on the blow-up:

$$(x, y, \lambda) \to (r^2\bar{x}, r^3\bar{y}, r^4v^4),$$

with $\bar{x}^2+\bar{y}^2+v^2 = 1$ (or $(\bar{x}, \bar{y}, v) \in \partial B$ where B is some "box" homeomorphic to D^3); we also restrict to $v \geq 0$. Working with v^4 instead of v is not really necessary, but is introduced here in order to fully agree with [7], where other parameters also had to be considered, imposing in a natural way that choice of the exponent.

The blown-up locus $\{r = 0\}$, for $v \geq 0$, is a half-sphere like in Figure 6(a) that we can also see from above like in Figure 6(b).

Again what we represent in Figure 6 is the desingularized field $\bar{X}_\lambda = \frac{1}{r}\hat{X}_\lambda$, that we obtain by blow-up and rescaling time. The field $\hat{X}_\lambda$, obtained by merely blowing-up, is equivalent to $\bar{X}_\lambda$ outside $\{r = 0\}$, but is identically zero on $\{r = 0\}$. The blowing-up $\hat{f}_\lambda$ of the (three-dimensional) diffeomorphism f_λ is equal to the identity on $\{r = 0\}$ and is infinitely near the time-one mapping of $\hat{X}_\lambda$ along $\{r = 0\}$.

As is usual in working on a sphere, the calculations will be made in different charts. For instance, for making calculations in the interior of the half sphere in the blow-up locus, we use $v = 1$ leading to an r-family of vector fields

$$\bar{y}\frac{\partial}{\partial \bar{x}} + (\bar{x}^2 + 1 + O(r))\frac{\partial}{\partial \bar{y}}.$$

Let us remark that on $\{v = 0\}$ we recover the two-dimensional situation described in Subsection 2.2. Possibly up to an extra C^∞ coordinate change (see [6]) we can suppose that f_0 is the time-one map of the vector field X_0. We again consider C and D as in Theorem 2.5, or more precisely, for each λ we consider $C \times \{\lambda\}$ and $D \times \{\lambda\}$, that for simplicity we still denote C and D, respectively, not specifying the λ-level.

We have seen in Theorem 2.5 that for N sufficiently large the iterates $f_0^N(C)$ will cut D in a transverse way at exactly two points (restricting our attention to a given neighbourhood of $(0, 0)$). Let us fix such N_0 and choose some $\lambda_0 > 0$ such that for all $0 \leq \lambda \leq \lambda_0$, the same property holds for $f_\lambda^{N_0}(C)$ with respect to D.

We can also take $\lambda_0 > 0$ small enough such that for all $0 \leq \lambda \leq \lambda_0$ the vector field X_λ is transverse to $f_0^N(C)$ as depicted in Figure 7(a) pointing

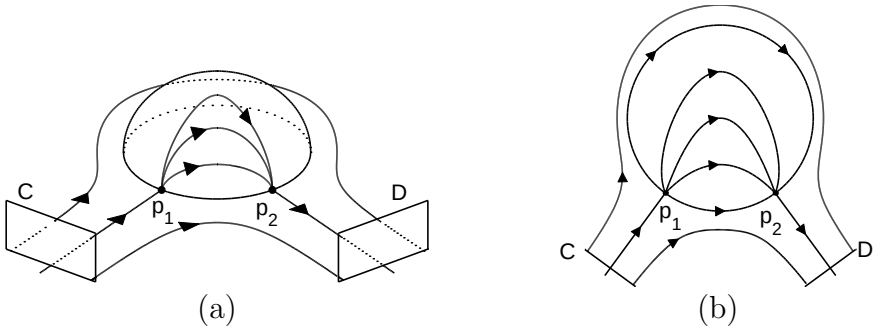

Figure 6: Blowing-up of X_λ.

inward the open disc R_N bounded by $f_0^N(C)$ and D.

Let $D_N^\lambda \subset R_N$ denote the closed part of R_N in between $f_\lambda^{-1}(D)$ and D. It is clear that for each $\lambda \in [0, \lambda_0]$ and for each $x \in R_N \setminus D_N^\lambda$ we still have $f_\lambda(x) \in R_N$, while $f_\lambda(x) \notin R_N$ if we take $x \in D_N^\lambda$ (to be sure about the last statement and since we have not paid attention to $f_\lambda \mid D_N^\lambda$ till now, it might be safer to change D by $f_0^{-1}(D)$, calling it D again).

In the further study of $f_\lambda^{N'}(C)$ we will restrict to $\lambda \in [0, \lambda_0]$, $N' > N$ and to the part of $f_\lambda^{N'}(C)$ inside R_N. By taking $\lambda_0 > 0$ smaller —if necessary— we can suppose that $f_\lambda^{N+1}(C) \cap (R_N \setminus D_N^\lambda) \neq \emptyset$.

We will now prove that for each $\lambda \in (0, \lambda_0]$ there is some $N_\lambda > N$, such that

$$f_\lambda^{N'}(C) \cap R_N \neq \emptyset \qquad \text{for } N+1 \leq N' \leq N_\lambda$$
$$f_\lambda^{N_\lambda+1}(C) \cap R_N = \emptyset$$

We recall that for each $N' \geq N$ we define $f_\lambda^{N'+1}(C)$ as $f_\lambda(f_\lambda^{N'}(C) \cap R_N)$, keeping our attention to what happens inside R_N and avoiding recurrences through the complement of R_N.

We need $f_\lambda^{N_\lambda}(C) \cap R_N \subset D_N^\lambda$.

The proof of the existence of such N_λ will be done in the blown-up situation. In Figure 7(b) we represent C, D and the respective iterates after blowing-up, without putting a cap above the notation. In fact for $\lambda > 0$, the blow-up is a diffeomorphic change, sending the invariant planes $\{\lambda = \text{const.}\}$ to the leaves of a regular foliation defined by $\{r^4 v^4 = \text{const.}\}$. It will not lead to a misinterpretation in transferring the used quantities to these regular leaves, without changing the name.

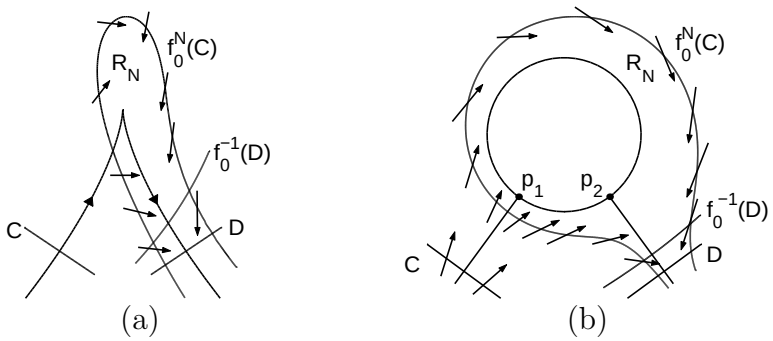

Figure 7: Delimiting a control region.

The reasoning which we will make is based on Figure 6 and on calculations made in [7]. We consider a neighbourhood of $\{r = 0\}$ containing R_N, that we further subdivide in three parts V_1, V_2 and V_3, defined in terms of $\bar{X}_\lambda$ (recall that $\bar{X}_\lambda = \frac{1}{r}\hat{X}_\lambda$). V_1 (resp. V_2) is an isolating block for the hyperbolic saddle point p_1 (resp. p_2), while in V_3 the vector field $\bar{X}_\lambda$ is a global flow box. We can choose the V_i compact in a way that V_1 and V_3, V_2 and V_3, as well as V_1 and V_2 overlap.

If the iterates of C, for $\lambda > 0$, would be considered with respect to the desingularized vector field $\bar{X}_\lambda$, then clearly after a sufficiently large time they would first leave V_1, and at the end lay completely in V_2 before leaving $V_1 \cup V_2 \cup V_3$. We only have to check that the same holds for $\hat{X}_\lambda = r\bar{X}_\lambda$, and also for f_λ which, along $\{r = 0\}$ is infinitely near the time-1 map of $\hat{X}_\lambda$.

Seen the compactness of the V_i, the verification can be done locally. Besides genuine flow boxes, both for $\hat{X}_\lambda$ and $\hat{f}_\lambda$, which we have for $r \neq 0$, we can encounter two different situations along $\{r = 0\}$.

The first is a "degenerate flow box" and the second a "degenerate hyperbolic saddle", occurring respectively at a point where $\bar{X}_\lambda \mid \{r = 0\}$ is non-singular or is singular, and hence, in the latter case, is a hyperbolic saddle.

In the first case it immediately follows from the flow box theorem that in well chosen coordinates (ξ, η, ζ), with $\{r = 0\}$ represented by $\{\zeta = 0\}$, the expressions of $\bar{X}_\lambda$ and $\hat{X}_\lambda$ are, respectively

$$\bar{X}_\lambda : \begin{cases} \xi' = 1 \\ \eta' = 0 \\ \zeta' = 0 \end{cases} \quad \text{and } \hat{X}_\lambda : \begin{cases} \xi' = \zeta A(\xi, \eta, \zeta) \\ \eta' = 0 \\ \zeta' = 0, \end{cases}$$

with $A(\xi, \eta, \zeta) > 0$. Accordingly $\hat{f}_\lambda$ can be given as an expression

$$\begin{cases} \xi \to \xi + \zeta B(\xi, \eta, \zeta) \\ \eta \to \eta + \zeta^N g(\xi, \eta, \zeta) \\ \zeta \to \zeta + \zeta^N h(\xi, \eta, \zeta), \end{cases}$$

with N arbitrarily big and $B(\xi, \eta, \zeta) > 0$. In fact the expression could be more simplified, if we would use that in the "family chart" ($\{v = 1\}$), $\hat{f}_\lambda$ respects the foliation $\{r = \text{const.}\}$, while in the "phase directional charts" ($\{\bar{x} = \pm 1\}$ or $\{\bar{y} = \pm 1\}$) it respects the foliation $\{rv = \text{const.}\}$. There is however no use to do so. It is immediate to observe that the coordinate ξ

defines a global Lyapunov function for $\bar{X}_\lambda$, but also for $\hat{X}_\lambda$ and $\hat{f}_\lambda$ as long as we keep $\lambda > 0$.

To work near $p_{1,2}$, the singularities of $\bar{X}_\lambda$ on $\{r = 0\}$, we use a "phase directional" chart given by $\{\bar{x} = 1\}$. We will restrict to a study near p_1, the calculations near p_2 being similar. We will also avoid making unnecessary calculations and only consider the essential facts. We know that $\bar{X}_\lambda$ has a hyperbolic saddle at p_1, whose unstable manifold is contained in the singular locus $\{r = 0\}$. As such the r-component of $\bar{X}_\lambda$ can be written as

$$r' = rA(r, v, \bar{y})$$

with $A(r, v, \bar{y}) < 0$, and $\hat{X}_\lambda$ has an r-component

$$r' = r^2 A(r, v, \bar{y}).$$

By this it is clear that the r-component on $\{r > 0\}$ is a Lyapunov function for $\bar{X}_\lambda$, $\hat{X}_\lambda$ and also for $\hat{f}_\lambda$, since the last is infinitely near the time-one mapping of $\hat{X}_\lambda$ along $\{r = 0\}$.

By the construction we know that $\{rv = \text{const.}\}$ is an invariant foliation both for $\hat{X}_\lambda$ and $\hat{f}_\lambda$. As such for $\lambda > 0$, while the r-component of $\hat{f}_\lambda$ is strictly decreasing, the v-component will be strictly increasing until exceeding the boundary of the chosen neighbourhood of p_1.

Going back now to the original f_λ and applying the previous observations on the forward iterates of C and the backward iterates of D, we can again use the time reversibility of f_λ under the mapping $(x, y, n) \to (x, y, -n)$. We know that γ_u is the mirror image of γ_s under the reflection $(x, y) \to (x, -y)$ and we can again ask D to be the mirror image of C under the same reflection. As such $f_\lambda^n(C)$ and $f_\lambda^{-n}(\mathrm{D})$ will also be mirror images under this reflection. We have seen that for each $\lambda > 0$ sufficiently small, there exists some N_λ such that $f_\lambda^{N_\lambda}(C) \cap R_N \subset D_N^\lambda$ implying that $f_\lambda^{N_\lambda}(C)$ is completely in $\{y > 0\}$. In keeping the same N_λ and taking $\lambda' \in (0, \lambda]$, we obtain curves that start at $f_\lambda^{N_\lambda}(C)$ for $\lambda' = \lambda$ and tend in a continuous way to $f_0^{N_\lambda}(C)$ for $\lambda' \to 0$. Certainly $f_0^{N_\lambda}(C)$ contains points in $\{y < 0\}$, as we have seen in the preceding paragraph.

Hence in $(0, \lambda]$ there must be a value λ' where $f_{\lambda'}^{N_\lambda}(C)$ is tangent to the x-axis. We hence have proven the existence of a sequence $\lambda_n \downarrow 0$ at which, for some $N_n \in \mathbb{N}$, there is a tangency between $f_{\lambda_n}^{N_n}(C)$ and $f_{\lambda_n}^{-N_n}(D)$. $\square$

In Figure 8 we represent the most probable situation, in which the two curves $f_{\lambda_n}^{N_n}(C)$ and $f_{\lambda_n}^{-N_n}(D)$ meet at exactly one point with a quadratic

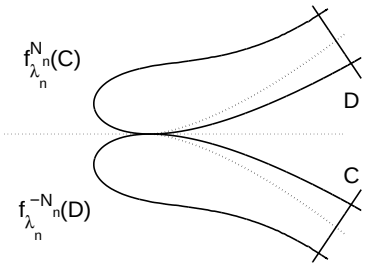

Figure 8: Contact between iterates of C and D.

tangency. This is most likely to be the case, but a precise proof might be technically quite involved.

2.4 Proof of Theorem 1.5

The assertion of Theorem 1.5 now follows easily from Theorem 2.6. Let γ_0 be the saddle-node periodic orbit associated to the cusp-transverse heteroclinic chain, and denote by Π_λ the Poincaré map along γ_0 parameterized by λ. Choosing the transverse section Σ appropriately, Π_λ is a family of planar diffeomorphisms, reversible under the restricted involution $\tilde{R} : (y, z) \mapsto (y, -z)$. As observed in Introduction, the Jacobian matrix $D\Pi_{\lambda_0}(p_0)$ at the saddle-node fixed point p_0 corresponding to γ_0 must have a double eigenvalue 1.

Moreover, it is assumed that the saddle-node periodic orbit is generically unfolded by the family X_λ, which is equivalent to saying that $D\Pi_{\lambda_0}(p_0)$ is conjugate to the unipotent matrix (1.3) as well as all the genericity conditions imposed in Theorem 2.3. From the condition (C3), the segments given by $C = W^u(P_+) \cap \Sigma$ and $D = W^s(P_-) \cap \Sigma$ intersect transversely with the stable set γ^s and the unstable set γ^u of γ_0.

All the hypotheses in Theorem 2.6 are thus satisfied, and hence there exists a sequence of parameters $\{\lambda_n\}$ converging to λ_0, which can be chosen to be monotone, and a sequence of integers $\{N_n\}$ diverging to ∞ such that $\Pi^{N_n}_{\lambda_n}(C)$ and $\Pi^{N_n}_{\lambda_n}(D)$ have a point of tangency. This means that for each λ_n the corresponding vector field X_{λ_n} has an orbit Γ_n along which $W^u(P_+)$ and $W^s(P_-)$ intersect tangentially. Moreover, since $N_n \to \infty$ as $n \to \infty$, the length of Γ_n diverges inside any a priori given tubular neighbourhood of the saddle-node periodic orbit. This completes the proof of Theorem 1.5. $\square$

3 Unfolding of a reversible Bykov cycle

In this section, we prove Theorem 1.13. We shall prove the condition (C1) in Subsection 3.1 and (C2) in Subsection 3.2.

3.1 Poincaré map along the reversible Bykov cycle

We describe the Poincaré map along the reversible Bykov cycle by using Shil'nikov's idea, in particular, what is called the exponential expansion. See [10] and references therein.

The Poincaré map along the heteroclinic cycle can be given by composing local transition maps near $P_\pm$ and global transition maps between them. In order to take the most advantage of the reversibility, which is the special feature of the system under consideration, we assume without loss of generality that the linear involution for reversibility is given by $R : (x, y, z) \mapsto (-x, y, -z)$ and take two-dimensional cross sections Σ_0 and Σ_1 to the cycle in such a way that they are contained in an R-invariant plane containing $\mathrm{Fix}(R)$, say the (y, z)-plane, and that Σ_0 has non-empty transverse intersection with the codimension zero heteroclinic orbit $W^s(P_-) \cap W^u(P_+)$ when $\lambda = \lambda_\infty$, whereas Σ_1 has non-empty transverse intersection with the codimension one heteroclinic orbit Γ.

Let $\varphi : \Sigma_0 \to \Sigma_1$ be the flow-defined transition map (with an appropriate domain of definition in Σ_0), and let $\psi : \Sigma_0 \to \Sigma_1$ be similarly defined by the time-reversed flow. The Poincaré map is then given by $\Pi = \psi^{-1} \circ \varphi$, and therefore, finding a fixed point of the Poincaré map is equivalent to finding a point $p \in \Sigma_0$ that satisfies $\varphi(p) = \psi(p)$.

Recall that the system is time-reversible with respect to the involution $R : (x, y, z) \mapsto (-x, y, -z)$, which fixes both Σ_0 and Σ_1. This implies that the maps φ, ψ are related by $\tilde{R} \circ \varphi \circ \tilde{R} = \psi$, where $\tilde{R} : (y, z) \mapsto (y, -z)$. This follows from the fact that the flow Φ^t of a reversible vector field is reversible in the sense that $R \circ \Phi^t \circ R = \Phi^{-t}$.

Since the codimension zero heteroclinic orbit persists under parameter variation and since $W^s(P_-)$ and $W^u(P_+)$ intersect transversely along it, it is more convenient to introduce coordinates (u, v) on Σ_0 such that the u-axis coincides with $W^u(P_+) \cap \Sigma_0$ and the v-axis does with $W^s(P_-) \cap \Sigma_0$. More precisely, we may assume, without loss of generality, that $W^u(P_+) \cap \Sigma_0$ is a smooth curve given by $G(y, z) = 0$ with $\mathrm{grad} G \neq 0$, and hence $W^s(P_-) \cap \Sigma_0$ can be given by $G(y, -z) = 0$ due to the reversibility. We then define the

new coordinates (u, v) as

$$u = G(y, z), \qquad v = G(y, -z).$$

These relations indeed define the new coordinates near the intersection point of $W^u(P_+)$ and $W^s(P_-)$ in Σ_0, because of the transversality of these invariant manifolds. Moreover, since the involution $\tilde{R}$ sends (y, z) to $(y, -z)$, it acts on the coordinates (u, v) as $T(u, v) = (v, u)$.

We fix such cross sections as well as the coordinates (u, v) on Σ_0 and (y, z) on Σ_1 using changes depending on the bifurcation parameter $\mu = \lambda - \lambda_\infty$. Under these circumstances, the above relation becomes

$$\tilde{R} \circ \varphi \circ T = \psi, \tag{3.1}$$

where $T(u, v) = (v, u)$. An immediate consequence of this fact is that the Poincaré map $\Pi = \psi^{-1} \circ \varphi$ satisfies $T \circ \Pi \circ T = \Pi^{-1}$, since

$$\begin{aligned} T \circ \Pi \circ T &= T \circ (\psi^{-1} \circ \varphi) \circ T = T \circ (T \circ \varphi^{-1} \circ \tilde{R} \circ \varphi) \circ T \\ &= \varphi^{-1} \circ \tilde{R} \circ \varphi \circ T = \varphi^{-1} \circ \psi = \Pi^{-1}. \end{aligned}$$

Therefore Π is reversible under the reflection T.

We are looking for saddle-node periodic orbits, hence saddle-node fixed points of the Poincaré map Π, which are symmetric under the involution $R : (x, y, z) \mapsto (-x, y, -z)$ and which intersect $\mathrm{Fix}(R)$, namely, the y-axis. Note that there is a fixed point $p \in \Sigma_0$ of Π, if and only if $\varphi(p) = \psi(p)$. This together with the fact that $q = \varphi(p)$ lies in the fixed point subspace of $\tilde{R}$ implies that p must be on the fixed point subspace of T, namely the diagonal of the (u, v)-plane. Therefore, the point $p \in \Sigma_0$ is of the form (u, u) for some u, and the condition for existence of a symmetric periodic orbit is that the z-component of $\varphi(u, u)$ be equal to 0.

Take a cylindrical neighborhood around P_- whose coordinates (r, θ, ζ) are chosen such that (r, θ) are the polar coordinates on $W^s(P_-)$ and the ζ-axis corresponds to $W^u(P_-)$. Let $\Sigma^-_{\mathrm{side}} = \{(r, \theta, w) \mid r = \delta, |w| < \delta\}$ in the polar coordinates, and let $\Sigma^-_{\mathrm{top}} = \{(\xi, \eta, \zeta) \mid \zeta = \delta, \sqrt{\xi^2 + \eta^2} < \delta\}$ in the cartesian coordinates. Then the map φ can be decomposed into $\varphi = \varphi_2 \circ \Pi^-_{\mathrm{loc}} \circ \varphi_1$, where $\Pi^-_{\mathrm{loc}} : \Sigma^-_{\mathrm{side}} \to \Sigma^-_{\mathrm{top}}$, and $\varphi_1 : \Sigma_0 \to \Sigma^-_{\mathrm{side}}$, $\varphi_2 : \Sigma^-_{\mathrm{top}} \to \Sigma_1$ are flow-defined local diffeomorphisms along (part of) heteroclinic orbits at $\lambda = \lambda_\infty$. Therefore the essential information of the map φ lies in the description of the local transition map Π^-_{loc}. This is given by the following Proposition, which is an immediate consequence of Theorem 1.6 of Deng [2]:

Proposition 3.1 *Under an appropriate choice of coordinates, the local transition map* $\Pi^-_{\rm loc} : \Sigma^-_{\rm side} \to \Sigma^-_{\rm top}$ *can be given by*

$$\begin{pmatrix} \theta \\ w \end{pmatrix} \mapsto \begin{pmatrix} \xi \\ \eta \end{pmatrix} = \begin{pmatrix} \delta w^\nu \cos(\theta + \Theta) + S_1(\theta, w; \mu) \\ \delta w^\nu \sin(\theta + \Theta) + S_2(\theta, w; \mu) \end{pmatrix},$$

where $\nu = |\lambda_s/\lambda_u|$ *and* $\Theta = -\frac{\omega_s}{\lambda_u} \log w$ *with* $\lambda_u (> 0)$ *and* $\lambda_s \pm \omega_s \sqrt{-1}$ $(\omega_s > 0)$ *being the eigenvalues of the linearized vector field at* P_-*. The remainder term* $S_i(\theta, w)$ $(i = 1, 2)$ *is a smooth function for* $w > 0$ *that satisfies*

$$\left| \frac{\partial^{k+\ell+m}}{\partial\theta^k \partial w^\ell \partial\mu^m} S_i(\theta, w; \mu) \right| \le C w^{\nu+\sigma-\ell},$$

where C *and* σ *are some positive constants,* k, ℓ, m *are non-negative integers.*

Remark 3.2 In Deng's paper, the result is given in terms of the so-called Shilnikov variables (t, τ, x_0, y_1) which in our notation correspond to

$$(t, \frac{1}{\lambda^u} \log(\frac{\delta}{w}), (\delta \cos\theta, \delta \sin\theta), \delta).$$

Deng's Theorem 1.6 asserts the existence of the exponential expansions for both the stable variable (x in Deng's paper) and the unstable variable (y) in terms of the Shil'nikov variables. The local transition map is then given by setting $t = 0$ for the unstable variable, and $t = \tau$ for the stable variable respectively, from which we obtain the above results. It is also used later in the bifurcation analysis of a reversible Bykov cycle. Note that a better estimate under a stronger eigenvalue condition is obtained by Homburg [10, Proposition 2.4].

Since the coordinates (u, v) in Σ_0 parametrize $W^u(P_+) \cap \Sigma_0$ and $W^s(P_-) \cap \Sigma_0$ respectively, and since $W^s(P_-) \cap \Sigma^-_{\rm side}$ corresponds to the plane $\{w = 0\}$ in (r, θ, w)-coordinates around P_-, the transition map $\varphi_1 : \Sigma_0 \to \Sigma^-_{\rm side}; (u, v) \mapsto (\theta, w)$ is such that $w = u\{1 + O(|u| + |v|)\}$ up to reparametrization of the coordinates if necessary, and hence

$$\begin{aligned} w^\nu &= O(1) \cdot u^\nu \\ -\frac{\omega_s}{\lambda_u} \log w &= -\frac{\omega_s}{\lambda_u} \log u + O(1). \end{aligned}$$

On the other hand, since the vanishing of the z-component of $\varphi_2(0,0) \in \Sigma_1$, denoted by $[\varphi_2(0,0)]_z$, means the existence of a codimension one heteroclinic orbit from P_- to P_+, $[\varphi_2(0,0)]_z$ is locally diffeomorphic to the bifurcation parameter μ. Namely, again up to reparametrization if necessary,

$$[\varphi_2(\xi,\eta)]_z = \mu + O(|\xi| + |\eta|),$$

which must be zero if (ξ,η) corresponds to a reversible periodic orbit. Combining

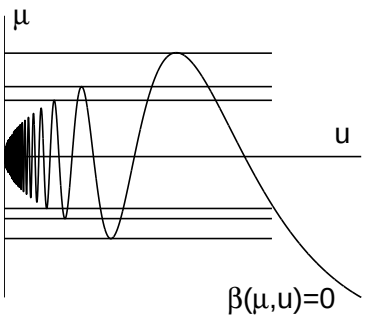

Figure 9: The solution curve $\beta(\mu,u) = 0$ for reversible periodic orbits.

these with the above proposition, the equation for reversible periodic orbits is given by

$$\beta(\mu,u) = \mu + u^\nu \cdot A\cos(-\frac{\omega_s}{\lambda_u}\log u + B) + S = 0,$$

where $A, B = O(1)$, and S satisfies the same type of estimates with respect to u as S_i in Proposition 3.1 does with respect to w, in particular, $S = O(u^{\nu+\sigma})$. It is then easy to show that the solution curve of $\beta(\mu,u) = 0$ is given asymptotically by the projection of a logarithmic spiral centered at $(\mu,u) = (0,0)$ that corresponds to the codimension one heteroclinic cycle. Notice that the envelop of the curve $\beta(\mu,u)$ is asymptotically of $O(u^\nu)$, and hence, the curve appears as in Figure 9. Therefore there are infinitely many saddle-node bifurcation points $\{\mu_n\}$ with $\mu_n \to 0$ which are given by the tangency points of the curve $\beta(\mu,u) = 0$ with the lines parallel to the u-axis in the (μ,u)-plane (see Figure 9). This concludes that saddle-node periodic orbits satisfying the condition (C1) accumulate to the reversible Bykov cycle.

3.2 Genericity of the reversible saddle-node bifurcations

In this subsection, we prove the genericity condition (C2) for the saddle-node periodic orbits obtained in the previous subsection, based on the hypotheses (B1) and (B2).

Let $\Pi(u, v, \mu)$ be the planar diffeomorphism on the (u, v)-plane Σ_0 obtained as the Poincaré map along a periodic orbit corresponding to a fixed point, and suppose that, when $\mu = \mu_0$, the fixed point $p = (u_0, u_0)$ represents a (reversible) saddle-node. As seen before, the Poincaré map Π can be written as $\psi^{-1} \circ \varphi$ where $\varphi, \psi : \Sigma_0 \to \Sigma_1$. We first consider whether the Jacobian matrix $D\Pi(p)$ at the fixed point p is conjugate to the unipotent matrix

$$\begin{pmatrix} 1 & 1 \\ 0 & 1 \end{pmatrix}.$$

Because of the reversibility, $D\Pi(p)$ at a saddle-node fixed point p must have double eigenvalue 1. Therefore if $D\Pi(p)$ is not conjugate to the above unipotent matrix, it must be conjugate to the identity matrix, hence $D\Pi(p) = I$. It follows from this and the form $p = (u_0, u_0)$ that the matrices $D\varphi(p)$ and $D\psi(p)$ must be identical. Suppose this is the case, then the relation (3.1) implies that $D\varphi(p) = D\psi(p)$ must take the form $\begin{pmatrix} a & a \\ b & -b \end{pmatrix}$ for some non-zero $a, b \in \mathbb{R}$. Since p corresponds to a saddle-node periodic orbit satisfying the condition (C1), it follows that the point p has to be in the symmetry axis of the involution R, namely the diagonal line in the (u, v)-plane, and that its images under φ and ψ are both tangent to the y-axis at the common image point $\varphi(p) = \psi(p)$. Therefore the vector given by

$$D\varphi(p) \begin{pmatrix} 1 \\ 1 \end{pmatrix} = D\psi(p) \begin{pmatrix} 1 \\ 1 \end{pmatrix}$$

is horizontal, i.e. lower component being zero, hence the lower row vector of $D\varphi(p) = D\psi(p)$ must be of the form $(b, -b)$ for some $b \neq 0$ as above.

However, as we will see, the upper row vector of $D\varphi(p) = D\psi(p)$ cannot be of the form (a, a), i.e. orthogonal to $(b, -b)$. If it were the case, then $D\varphi(p)\mathbf{e}_- = D\psi(p)\mathbf{e}_-$ would be vertical, i.e. orthogonal to $D\varphi(p)\mathbf{e}_+ = D\psi(p)\mathbf{e}_+$, where

$$\mathbf{e}_+ = \begin{pmatrix} 1 \\ 1 \end{pmatrix}, \qquad \mathbf{e}_- = \begin{pmatrix} 1 \\ -1 \end{pmatrix}.$$

Let us now show that this is impossible for $D\varphi(p)$. A similar reasoning also applies to $D\psi(p)$. For that purpose, we suppose, without loss of generality, that the domain of definition of the map φ is in $\{u \geq 0\}$ in Σ_0, and, along the diagonal $\Delta = \{(u,u) \mid u \in \mathbb{R}\}$ in the (u,v)-plane Σ_0, we consider the lines $C_{u_0} = \{(u, 2u_0 - u) \mid u \geq 0\}$ which are perpendicular to Δ. We will measure the angle of $D\varphi(p)\mathbf{e}_+$ and $D\varphi(p)\mathbf{e}_-$ by successively seeing how $D(\varphi_1)(p)$, $D(\Pi^-_{\rm loc})(\varphi_1(p))$ and $D(\varphi_2)((\Pi^-_{\rm loc} \circ \varphi_1)(p))$ change the angle between $\mathbf{e}_+$ and $\mathbf{e}_-$.

In keeping $p = (u,u)$ with $u \geq 0$ to a sufficiently small neighborhood of $(0,0)$, we know that $D(\varphi_1)(p)$ changes the angle with a factor $k(p)$ that is bounded away from 0 and $+\infty$ in a uniform manner, since it is a regular local diffeomorphism. We then see the effect of $D(\Pi^-_{\rm loc})(\varphi_1(p))$ on the angle between $D(\varphi_1)(p)\mathbf{e}_+$ and $D(\varphi_1)(p)\mathbf{e}_-$. On $\Sigma^-_{\rm side}$, we consider the images of Δ and C_{u_0} under φ_1. The curves $\varphi_1(\Delta)$ and $\varphi_1(C_{u_0})$ are smooth curves, which cut $\{w = 0\}$ transversely. Let $D_1 = \{\theta = \theta_1(w)\}$ represent $\varphi_1(\Delta)$, while $D_2 = \{\theta = \theta_2(w)\}$ represents any of $\varphi_1(C_{u_0})$. Suppose $\theta_1(0) = \theta_*$. In the following calculations, we will restrict the curves $D_1 = \varphi_1(\Delta)$ and $D_2 = \varphi_1(C_{u_0})$ in a fixed neighborhood $V = [\theta_* - \varepsilon, \theta_* + \varepsilon] \times [0, w_0]$ with $\varepsilon > 0$ and $w_0 > 0$ sufficiently small. It corresponds to a fixed (small) neighborhood of $(0,0)$ in the (u,v)-plane with $u \geq 0$.

If $q = \varphi_1(p)$ is a point of intersection of D_1 and D_2 in V, then the angle of $D(\varphi_1)(p)\mathbf{e}_+$ and $D(\varphi_1)(p)\mathbf{e}_-$ is given by the angle of $\frac{d\theta_1}{dw}(\bar{w})$ and $\frac{d\theta_2}{dw}(\bar{w})$, if $q = (\theta_1(\bar{w}), \bar{w}) = (\theta_2(\bar{w}), \bar{w})$. We will estimate the angle between $\Pi^-_{\rm loc}(D_1)$ and $\Pi^-_{\rm loc}(D_2)$ at $\Pi^-_{\rm loc}(q)$ by using Proposition 3.1. The curves D_i $(i = 1,2)$ are transformed to $E_i = \Pi^-_{\rm loc}(D_i)$, which is given by a parametric expression $(\xi, \eta) = (\xi(w), \eta(w))$ with

$$\begin{aligned} \xi(w) &= \delta w^\nu \cos(\theta_i(w) + \Theta(w)) + S_1(\theta_i(w), w; \mu) \\ \eta(w) &= \delta w^\nu \sin(\theta_i(w) + \Theta(w)) + S_2(\theta_i(w), w; \mu), \end{aligned}$$

where $\Theta(w) = -(\omega_s/\lambda_u)\log w$. The tangent vector of E_i at a point $(\xi(w), \eta(w))$ has an expression $Z_i(w) = (Z_i^\xi(w), Z_i^\eta(w))$ $(i = 1,2)$ given by

$$\begin{aligned} Z_i^\xi(w) &= \delta\{\nu \cos(\theta_i(w) + \Theta(w)) + \frac{\omega_s}{\lambda_u} \sin(\theta_i(w) + \Theta(w))\} w^{\nu-1} + o(w^{\nu-1}) \\ Z_i^\eta(w) &= \delta\{\nu \sin(\theta_i(w) + \Theta(w)) - \frac{\omega_s}{\lambda_u} \cos(\theta_i(w) + \Theta(w))\} w^{\nu-1} + o(w^{\nu-1}). \end{aligned}$$

Here we have used the fact that $\theta_i(w)$ and its derivative are uniformly bounded. The inner product of $Z_1(w)$ and $Z_2(w)$ at $q = (\theta_1(\bar{w}), \bar{w}) =$

$(\theta_2(\bar{w}), \bar{w})$ thus becomes

$$\delta^2 \left(\nu^2 + \frac{\omega_s^2}{\lambda_u^2} \right) \cos(\theta_1(\bar{w}) - \theta_2(\bar{w})) \bar{w}^{2(\nu-1)} + o(\bar{w}^{2(\nu-1)}),$$

and dividing it by the length of these vectors gives the cosine of the angle between $Z_1(\bar{w})$ and $Z_2(\bar{w})$ as

$$\cos(\theta_1(\bar{w}) - \theta_2(\bar{w})) + o(1) = 1 + o(1),$$

which can be made as close to 1 as required by taking ε and w_0 sufficiently small. In other words, the angle of these vectors, and hence the angle of $D(\Pi^-_{\rm loc} \circ \varphi_1)(p)\mathbf{e}_+$ and $D(\Pi^-_{\rm loc} \circ \varphi_1)(p)\mathbf{e}_-$ converges to zero as $p = (u, u)$ tends to the origin.

Since φ_2 is a local diffeomorphism near $(\xi, \eta) = (0, 0)$, it is clear that this property of the angle remains true for $D\varphi(p)\mathbf{e}_+ = D(\varphi_2 \circ \Pi^-_{\rm loc} \circ \varphi_1)(p)\mathbf{e}_+$ and $D\varphi(p)\mathbf{e}_- = D(\varphi_2 \circ \Pi^-_{\rm loc} \circ \varphi_1)(p)\mathbf{e}_-$. This proves that $D\varphi(p)\mathbf{e}_+$ and $D\varphi(p)\mathbf{e}_-$ cannot be orthogonal, and hence that $D\Pi(p)$ must be conjugate to the unipotent matrix.

The previous analysis also shows that, in (y, z)-coordinates on Σ_0 in which $\tilde{R}(y, z) = (y, -z)$, the fixed point set of $D\Pi(p)$ has to be the y-axis. Using the reversibility of $D\Pi(p)$ with respect to $\tilde{R}$ once again, we see that the matrix $D\Pi(p)$ has to be

$$\begin{pmatrix} 1 & c \\ 0 & 1 \end{pmatrix}$$

with $c \neq 0$. Linear change of z, if necessary, permits to suppose $c = 1$, and hence $D\Pi(p)$ is exactly given by

$$\begin{pmatrix} 1 & 1 \\ 0 & 1 \end{pmatrix}.$$

It remains to show the genericity conditions which are formulated as the following two conditions:

$$(1) \quad \frac{\partial [\Pi]_z}{\partial \mu}(y_0, z_0, \mu_0) \neq 0, \qquad (2) \quad \frac{\partial^2 [\Pi]_z}{\partial y^2}(y_0, z_0, \mu_0) \neq 0.$$

We give a proof of these conditions below.

First recall that the curve given by $\beta(\mu, u) = 0$ gives the condition for the existence of symmetric periodic orbits, and hence the points of tangency

on the curve with respect to the lines parallel to the u-axis correspond to the reversible saddle-node bifurcations. From the expression of $\beta(\mu, u)$ given in the previous subsection which shows that the curve is asymptotically the projection of a logarithmic spiral, it is clear that there is a sequence of such tangency points accumulating to $(0, 0)$, and moreover, the tangencies that are sufficiently close to $(0, 0)$ are quadratic. Therefore, in order to prove the non-degeneracy conditions (1) and (2) given above, it is enough to show only one of these, because the other follows from the quadratic nature of the tangency. Below we prove the condition (1) using the hypothesis (B2).

In order to prove (1), we note that the Poincaré map along the reversible saddle-node periodic orbit is close to that of the reversible Bykov cycle, if we choose the periodic orbit sufficiently close to the cycle. As a consequence, we will now see that the condition (B2) for the heteroclinic cycle implies the desired condition (1) for the periodic orbit. Recall that the Poincaré map for the heteroclinic cycle is given by composing maps which are either local transition maps near the saddle-focus equilibrium points or else transition maps along the heteroclinic orbits outside neighborhoods of the equilibrium points. Although the local transition maps around the equilibrium points depend on parameters, the description of the local transition maps does not change much under variation of parameters, because one can choose coordinates also depending on parameters. The transition map along the heteroclinic orbit from P_+ to P_- does not depend much on parameters either, because of the transversality. Therefore, the essential dependence of the Poincaré map on the parameter comes from the transition along the heteroclinic orbit from P_- to P_+ which is given by the coincidence of one-dimensional invariant manifolds $W^u(P_-)$ and $W^s(P_+)$. Then by the hypothesis (B2), we assume that this one-dimensional connection is broken in a non-degenerate way under the variation of the parameter μ around $\mu = 0$ corresponding to the presence of the reversible Bykov cycle. In particular, the derivative in z-direction with respect to the parameter should be non-zero, because it is transverse to the y-axis which is the fixed subspace of the involution R. This proves the non-degeneracy condition (1), and hence (2) also, as noted above, and therefore, the proof of Theorem 1.13 is completed. □

4 Discussions: Numerical results

Some numerical work can be done in order to support and illustrate many of the theoretical results and conjectures that have been presented in this paper. Following calculation has been done using the `MATLAB` tools [18]. Let us first present some numerical evidence for the occurrence of a cusp-transverse heteroclinic chain in the Michelson system.

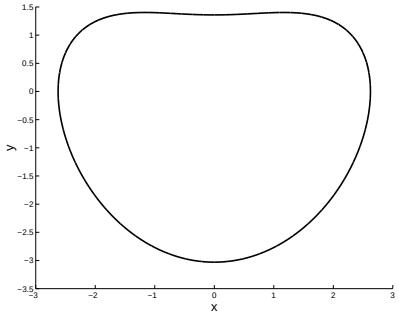

Figure 10: Projection on the plane $z = 0$ of the periodic orbit for $c = c_L$.

In [17] and [20], the authors obtained the approximate value $c_L \approx 1.2662$ as the parameter value for the occurrence of the first saddle-node periodic orbit. We have checked it and obtained a more accurate value by the following computation. We study the curve C given by the first intersection with the half-plane $\{x = 0,\, y > 0\}$ of the orbits with initial points on the negative y-axis; there is a segment l_0 on this axis for which such intersection is defined. The first saddle-node periodic orbit corresponds, for decreasing c, to the first tangency of C with the positive y axis. Let $m(c)$ be the minimum value of the z-coordinate along C, considered as a function of $y \in l_0$; the parameter c_L is given by the zero of $m(c)$ closest to 1.2662. With this method we get the value $c_L \approx 1.26623233$, for which $m(c_L) \approx -1.2 \times 10^{-15}$ and such a minimum is achieved for $y_L \approx -3.02959972$. In Figure 10, the projection on the xy-plane of the corresponding periodic orbit γ_L is plotted.

Consider now the Poincaré map $\Pi = ([\Pi]_y, [\Pi]_z)$ along γ_L defined on a cross section contained in the half-plane $\{x = 0,\, y < 0\}$. Let us now check numerically that the condition (C2) in Definition 1.4 is satisfied for the periodic γ_L. We have performed a numerical integration of the variational

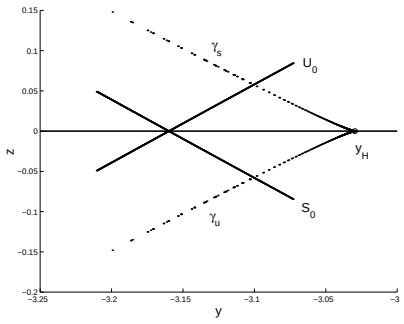

Figure 11: The global hypothesis for a cusp-transverse heteroclinic chain. U_0 and S_0 are pieces of the first intersections of $W^u(P_+)$ and $W^s(P_-)$, respectively, with the plane $x = 0$. γ_s and γ_u are branches of $W^s(H)$ and $W^u(H)$, respectively, where H denotes the hyperbolic saddle arising, at the selected parameter value, after the saddle-node bifurcation.

equations to compute the derivatives of Π and found:

$$\frac{\partial[\Pi]_{y,z}}{\partial(y,z)} \approx \begin{pmatrix} 1.0000 & 2.0537 \\ -1.3 \times 10^{-5} & 1.0000 \end{pmatrix} \approx \begin{pmatrix} 1.0000 & 2.0537 \\ 0.0000 & 1.0000 \end{pmatrix}$$
$$\frac{\partial[\Pi]_z}{\partial c} \approx -7.6896 \qquad \frac{\partial^2[\Pi]_z}{\partial y^2} \approx -6.3771 \times 10^2.$$

Note that all the local conditions for a cusp-transverse heteroclinic chain are, at least numerically, satisfied. We observe that the numerically computed Jacobian matrix of the Poincaré map along the periodic orbit γ_L is unipotent, and the genericity of the unfolding is also verified as seen above.

On the other hand, in order to verify the global hypothesis (C3), we have chosen a parameter value $c \lessapprox c_L$ and obtained an estimate of the hyperbolic saddle $H = (0, y_H, 0)$ which, for such a parameter value, appears in a saddle-node bifurcation. Figure 11 shows a numerical approach of the first intersections of $W^u(P_+)$ and $W^s(P_-)$ with the plane $\{x = 0\}$, and also of two branches of $W^s(H)$ and $W^u(H)$. Since such branches approach the stable and unstable sets, respectively, of the saddle-node point, we can expect that they are close enough to such sets. Hence we can consider Figure 11 as a support of the validity of (C3), at least for the Lau's parameter value c_L. To approximate $W^u(H)$, we have used a second-degree local expansion of the Poincaré map at H, with coefficients obtained by integration of the variational equations, and a second-degree local expansion of the invariant

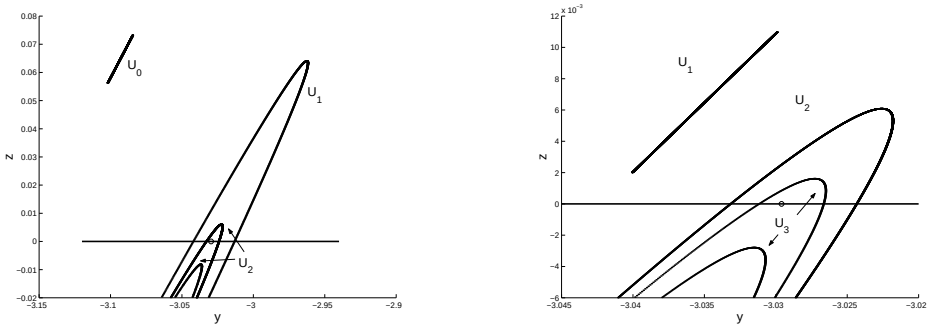

Figure 12: Intersections of $W^u(P_+)$ with the half-plane $\{x = 0,\, y < 0\}$ for $c = c_L$. U_0 is a piece of the first intersection and U_1, U_2 and U_3 are pieces of the subsequent iterates. The small circle on the y-axis corresponds to the fixed point given by the periodic orbit. Figure (b) is a magnification around such fixed point.

manifold. To draw the orbits in Figure 11 we take initial points (y, z) on the invariant manifold with $y \in [y_1, y_2]$, where $y_2 = y_H - 10^{-6}$ and y_1 is given by the y-coordinate of $\Pi(y_2, z_2)$ with (y_2, z_2) on the invariant manifold. Here and in the sequel, numerical approximation of $W^u(P_+)$ is obtained by using a 30th-degree local expansion to obtain good fundamental domains where initial conditions are taken. In Figure 12 we have plotted several intersections of $W^u(P_+)$ with the half-plane $\{x = 0,\, y < 0\}$ for $c = c_L$. It should be recalled that for this parameter value, the two-dimensional invariant manifolds have infinitely many intersections; we have only computed the first ones. Figure 13 shows the sequence of the first three tangent bifurcations.

Let us also present some numerical computations at the parameter value $c = c_K = 15\sqrt{22/19^3}$ at which we have coincidence of branches of the one-dimensional invariant manifolds ([13]) and at which it is conjectured that there exists a Bykov cycle. In Figure 14 we show such a cycle obtained numerically. The connection along the one-dimensional invariant manifolds has been plotted using the explicit solution from [13]. Choosing an appropriate fundamental domain of $W^u(P_+)$, parametrized by an angle θ, and considering the function $z(\theta)$ given by the value of the z-coordinate at the first intersection with the plane $x = 0$, we have approximated the zero of such

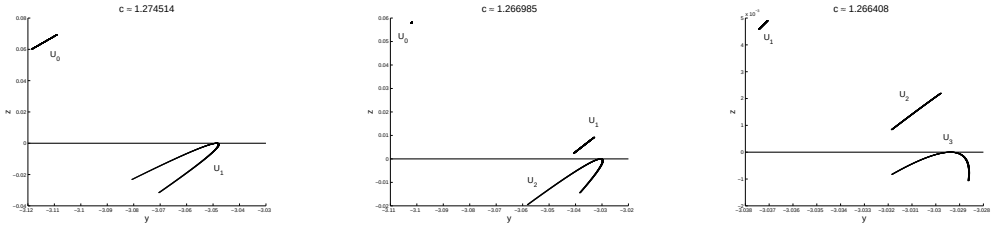

(a) (b) (c)

Figure 13: First three tangent bifurcations.

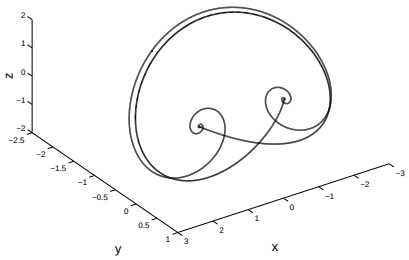

Figure 14: A Bykov cycle for $c = c_K$.

function. It leads to a heteroclinic connection crossing the y-axis at the point $(0, y_0, 0)$ with $y_0 \approx -2.17092839$.

In Figure 15(a) we have drawn the graph of the function $z(c)$ given by the value of the z-coordinate at the first intersection point of the one-dimensional invariant manifold $W^u(P_-)$ with the half-plane $\{x = 0, y < 0\}$. It is clear from that figure that condition (B2) in Definition 1.9 is satisfied. A numerical computation of the derivative at $c = c_K$ gives $\frac{\partial z}{\partial c} \approx -4.5185$. In Figure 15(b) we have drawn the first intersections U_0 and S_0 of the two-dimensional invariant manifolds $W^u(P_+)$ and $W^s(P_-)$, respectively, with the plane $x = 0$, in order to show the transversality. Numerically solving the variational equation we can approximate the tangent plane at the intersection point; we get $\frac{dz}{dy} \approx 0.8364$ along U_0. Figure 15(b) also includes a plot of the tangent

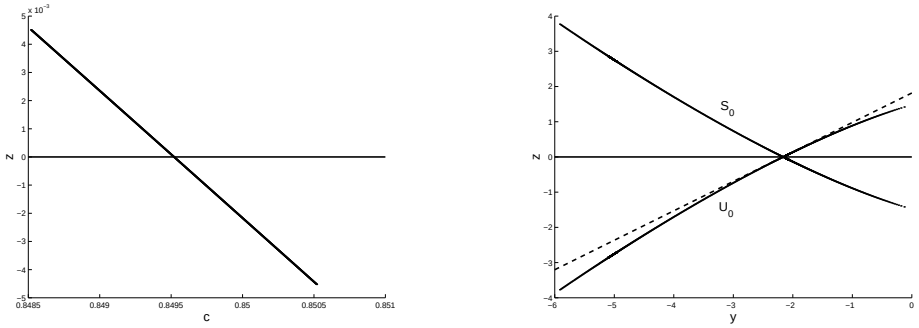

(a) (b)

Figure 15: In (a) we represent the value of the z-coordinate at the first intersection point of $W^u(P_-)$ with the half-plane $\{x = 0, y > 0\}$, as a function of the parameter. In (b) the first intersection of the two-dimensional invariant manifolds with the plane $x = 0$ is presented.

line.

Finally, we remark that Wilczak [24] has numerical results concerning the Michelson system which are related to our results. Some of his computations are made rigorous.

References

[1] V. V. Bykov, Bifurcations of dynamical systems close to systems with a separatrix contour containing a saddle-focus, in "Methods of the qualitative theory of differential equations", Russian original in 1980, English translation: Amer. Math. Soc. Trans. Ser. 2, **200** (2000), 87–97.

[2] B. Deng, Exponential expansion with Šil'nikov's saddle-focus, J. Diff. Eq. **82** (1989), 156–173.

[3] F. Dumortier, *Singularities of vector fields*, Monografias de Matematica, n. 32, IMPA, Rio de Janeiro, 1978.

[4] F. Dumortier, Non-stabilizable jets of diffeomorphisms in $\mathbb{R}^2$ and of vector fields in $\mathbb{R}^3$, Ann. of Math. **124** (1986), 405–440.

[5] F. Dumortier, S. Ibáñez and H. Kokubu, New aspects in the unfolding of the nilpotent singularity of codimension three, Dynamical Systems **16** (2001), 63–95.

[6] F. Dumortier, P. Rodrigues, and R. Roussarie, *Germs of Diffeomorphisms in the Plane*, Lect. Notes Math., Vol. 902, 1981, Springer-Verlag.

[7] F. Dumortier, R. Roussarie, and J. Sotomayor, Bifurcations of cuspidal loops, Nonlinearity **10** (1997), 1369–1408.

[8] F. Fernández-Sánchez, *Comportamiento dinámico y de bifurcaciones en algunas conexiones globales de equilibrio en sistemas tridimensionales*, Ph.D Thesis, University of Sevilla, 2002.

[9] P. Glendinning and C. Sparrow, T-points: a codimension two heteroclinic bifurcation, J. Stat. Phys. **43** (1986), 479–488.

[10] A. J. Homburg, Periodic attractors, strange attractors and hyperbolic dynamics near homoclinic orbits to saddle-focus equilibria, Nonlinearity **15** (2002), 1029–1050.

[11] S. Ibáñez and J. A. Rodríguez, Shil'nikov configurations in any generic unfolding of the nilpotent singularity of codimension three on $\mathbb{R}^3$, J. Diff. Eq. **208** (2005), 147–175.

[12] P. Kent and J. Elgin, Travelling-waves of the Kuramoto-Sivashinsky equation: period multiplyng bifurcations, Nonlinearity **5** (1992), 899–919.

[13] Y. Kuramoto and T. Tsuzuki, Persistent propagation of concentration waves in dissipative media far from thermal equilibrium, Prog. Theor. Phys. **55** (1976), 356–369.

[14] J. S. W. Lamb, *Reversing symmetries in dynamical systems*, Ph.D thesis, University of Amsterdam, 1994.

[15] J. S. W. Lamb and J. A. G. Roberts, Time-reversal symmetry in dynamical systems: A survey, Physica D **112** (1998), 1–39.

[16] J. S. W. Lamb, M.-A. Teixeira, and K. N. Webster, Heteroclinic bifurcations near Hopf-zero bifurcation in reversible vector fields in $\mathbb{R}^3$, J. Diff. Eq., in press.

[17] Y.-T. Lau, The "cocoon" bifurcations in three-dimensional systems with two fixed points, Int. J. Bif. Chaos **2** (1992), 543–558.

[18] MathWorks, `MATLAB` User's Guide, Natick MA USA, 1999, Version 5.3.

[19] C. K. McCord, Uniqueness of connecting orbits in the equation $Y^{(3)} = Y^2 - 1$, J. Math. Anal. Appl. **114** (1986), 584–592.

[20] D. Michelson, Steady solutions of the Kuramoto-Sivashinsky equation, Physica D **19** (1986), 89–111.

[21] F. Takens, Forced oscillations and bifurcations, in "Applications of Global Analysis 1", Comm. of Math. Inst. Rijksuniv., Utrecht, **3** (1974), 1-59; reprinted in "Global Analysis of Dynamical Systems" (Eds. H. Broer, B. Krauskopf, and G. Vegter), 2001, Institute of Physics Publishing, pp. 1–61.

[22] W. C. Troy, The existence of steady solutions of the Kuramoto-Sivashinsky equation, J. Diff. Eq. **82**, (1989) 269–313.

[23] J. B. van den Berg, S. van Gils, and T. Visser, Parameter dependence of homoclinic solutions in a single long Josephson junction, Nonlinearity **16** (2003), 707–717.

[24] D. Wilczak, Symmetric heteroclinic connections in the Kuramoto-Sivashinsky equations - a computer assisted proof, Preprint.